Ultraviolet and near-infrared femtosecond temporal pulse shaping with a new high-aspect-ratio one-dimensional micromirror array

Stefan M. Weber,[1,2,†] Jérôme Extermann,[1,*,†] Luigi Bonacina,[1,4] Wilfried Noell,[2] Denis Kiselev,[1] Severin Waldis,[3] Nico F. de Rooij,[2] and Jean-Pierre Wolf[1]

[1]*Université de Genève, GAP-Biophotonics, 20 rue de l'Ecole de Médecine, 1211 Genève 4, Switzerland*

[2]*EPFL/STI/IMT-NE/SAMLAB, Rue Jaquet-Droz 1, 2002 Neuchâtel, Switzerland*

[3]*Université de Neuchâtel, Rue Jaquet-Droz 1, 2002 Neuchâtel, Switzerland*

[4]*e-mail: luigi.bonacina@unige.ch*

**Corresponding author: jerome.extermann@unige.ch*

Received June 11, 2010; revised August 11, 2010; accepted August 12, 2010; posted August 20, 2010 (Doc. ID 129944); published September 9, 2010

We demonstrate the capabilities of a new optical microelectromechanical systems device that we specifically developed for broadband femtosecond pulse shaping. It consists of a one-dimensional array of 100 independently addressable, high-aspect-ratio micromirrors with up to 3 μm stroke. We apply linear and quadratic phase modulations demonstrating the temporal compression of 800 and 400 nm pulses. Because of the device's surface flatness, stroke, and stroke resolution, phase shaping over an unprecedented bandwidth is attainable. © 2010 Optical Society of America

OCIS codes: 230.4040, 230.4685, 320.2250, 320.5540.

During the past decade, numerous applications of coherent control, controlling quantum processes with light, have been reported, based either on close-loop [1] or open-loop [2] schemes. For many researchers, one of the long-term ambitions is to efficiently control the dynamics of biologically relevant molecules via phase-sensitive schemes with some first promising results [2–6]. So far, one of the principal obstacles has been the fact that most of the absorption bands of biomolecules lie in the UV, a spectral region hardly accessible by transmissive devices. This contingency has stimulated a series of alternative schemes (e.g., indirect shaping [7]) and of technological progresses encompassing all the available technologies of spatial light modulators (SLMs): the application range of acousto-optical modulators has been successfully extended to the UV–visible region [8–11], and new liquid crystals have been introduced for extending the spectral transmission of such devices in the UV [12]. As an alternative approach, reflective microelectromechanical systems (MEMS) have proven their broadband applicability for femtosecond pulse shaping [13–15], even in the deep UV [16,17].

In this Letter, we demonstrate the extensive wavelength range of an MEMS device by performing phase-shaping at 800 and 400 nm. The motivation for our development was to specifically design a system for femtosecond pulse shaping with dedicated optical and electromechanical properties for our application [16]: (i) a high duty cycle, (ii) low diffraction losses, (iii) large strokes, and (iv) low power densities. These design specifications could be achieved by (i) an external electronics able to indefinitely hold a specific mirror stroke, (ii) minimizing the gaps between mirrors to achieve a fill factor of about 98%, (iii) using a novel double-spring design in combination with electrostatic vertical comb drive actuators [18,19], and (iv) employing 120 μm $\times$ 1000 μm-long, high-aspect-ratio mirrors.

The mirror array, including the electrostatic actuators, the springs, and the wire bonds are depicted in Fig. 1(a). The device is bulk-micromachined from a silicon-on-insulator wafer with a 35-μm-thick device layer using delayed-mask deep reactive ion etching. Utilizing a patterning of the back side, the micromirrors could be released without release holes, thus reducing diffraction sources to a minimum. The mirrors are coated with a 10/300 nm Ti/Al layer. Because of the 35-μm-thick device layer, the damage threshold is equivalent to a standard aluminum coating. A custom electronics (containing multiple AD5535 DA converters with 14 bit precision and 200 V maximal output) delivers the driving voltages. An individual pixel calibration (by white-light interferometry with a Veeco/Wyko NT1100 DMEMS) was necessary to compensate for the residual, overall chip bow of about 1.5 μm. The stroke measured at the maximal voltage applied for these measurements (70 V) was 3 μm, which, considering the chip bow would, in principle, allow addressing wavelengths up to 3 μm with 12.5 bits

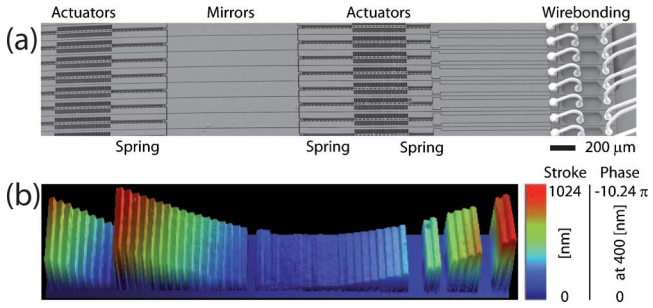

Fig. 1. (Color online) (a) SEM image of the high-aspect-ratio mirror array. The mirrors are fixed from each side by two springs connected to the vertical comb drive actuators. The wire bonds for electrical connectivity are visible on the right side. More details can be found in [19]. (b) White-light interferometry image of a set of actuated mirrors in a parabolic configuration.

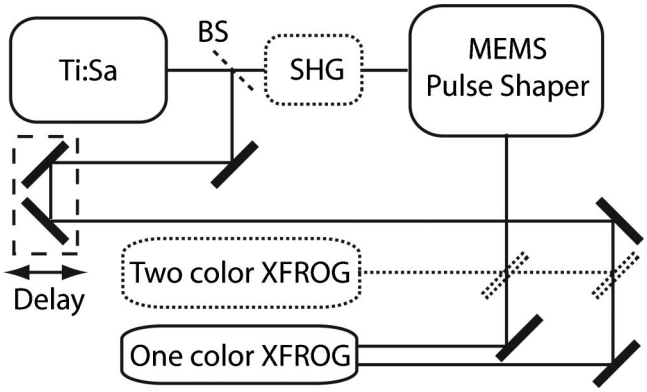

Fig. 2. Experimental Scheme: BS, 50/50 beam splitter.

resolution. It is worth pointing out that the stroke resolution affects the phase-resolution differently, according to the spectral region addressed. At 3 μm, the achievable phase-resolution is clearly tenfold that expected at 300 nm. Moreover, one has to take into account the surface roughness of individual mirrors, which could be estimated to be around $R_{aa} = 15$ nm.

For the optical measurements at $\lambda_0 = 800$ and 400 nm, femtosecond laser pulses were generated by a Femtosource Synergia 20 oscillator, delivering 15 fs pulses at 80 MHz repetition rate, centered at 800 nm (Fig. 2). Directly after the oscillator, the gate pulse (FWHM: $\Delta\lambda = 58$ nm and $\Delta\tau = 18$ fs) was extracted for characterization purposes with a 50/50 broadband beam splitter. For the $\lambda_0 = 400$ nm measurements, the transmitted beam was doubled in a 500-μm-thick beta barium borate (BBO) crystal. Successively, the beam entered the pulse shaper, composed by a folded, $4f$ dispersion-free grating compressor [20] with a 600 lines/mm (respectively 1200 lines/mm) grating blazed at 800 nm (respectively 400 nm), and a cylindrical lens ($f = 150$ mm). To ensure that the beam was fully contained in the vertical direction, a second ($f = 60$ mm) cylindrical lens rotated by 90° was introduced to reduce the vertical spot size. For $\lambda_0 = 800$ nm pulse characterization, we performed one-color XFROG [21] employing a 10 μm thin BBO crystal to maximize the accessible bandwidth. For $\lambda_0 = 400$ nm, we used two-color XFROG with a 100-μm-thick third-harmonic crystal. The signals were detected by a spectrometer (Princeton Instruments, Acton, SP2300i) coupled either with an in-line CCD (Thorlabs LC1-USB) or a photomultiplier tube (Hamamatsu H7732). A Melles–Griot interferometric filter was used to extract the sum-frequency signals and remove traces of the pump pulse.

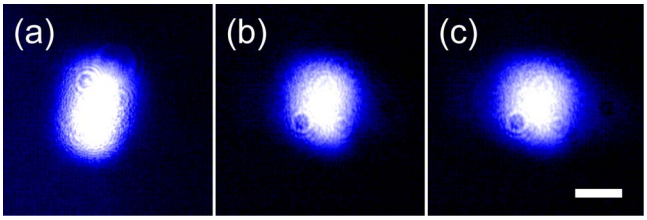

Fig. 3. (Color online) Spatial beam profile on a logarithmic intensity scale at $\lambda_0 = 400$ nm after the $4f$ setup with (a) a mirror replacing the SLM in the Fourier plane, (b) the MEMS micromirror device with a flat phase mask applied and (c) with a random phase mask. No diffraction pattern resulting from the SLM is observed. Scale bar: 2 mm.

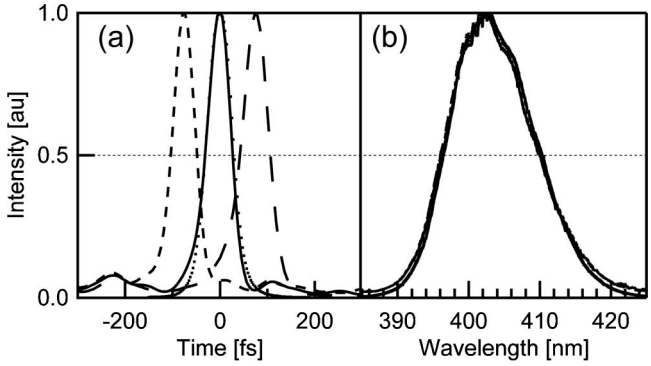

Fig. 4. (a) Phase-shaping with the MEMS micromirror device demonstrated at $\lambda_0 = 800$ nm for two opposite linear phase masks, (b) corresponding to a pulse shift of ± 73 fs (cross correlations, dashed curves) without modifying the pulse spectra. Flat phase masks (solid) and 1″ mirror (dots) depict the unmodulated pulses.

The spatial beam profiles, measured with the Newport LBP-1 profiler, are rather homogeneous and display no evident effects of diffraction due to device pixelization even on a logarithmic plot (Fig. 3). A comparison [Fig. 3(a)], which was taken with a mirror replacing the SLM in the Fourier plane, underlines this observation. Taking into account the nominal grating reflectivity (70%) and the lens transmission (93%), the losses of the SLM device (diffraction and reflectivity) can be estimated to be below 15% at 800 nm. The overall measured throughput of the pulse shaper was 33% at this wavelength.

Figure 4 displays the nonnormalized results when a linear spectral phase is applied (at $\lambda_0 = 800$ nm), which delays the shaped pulse with respect to the reference

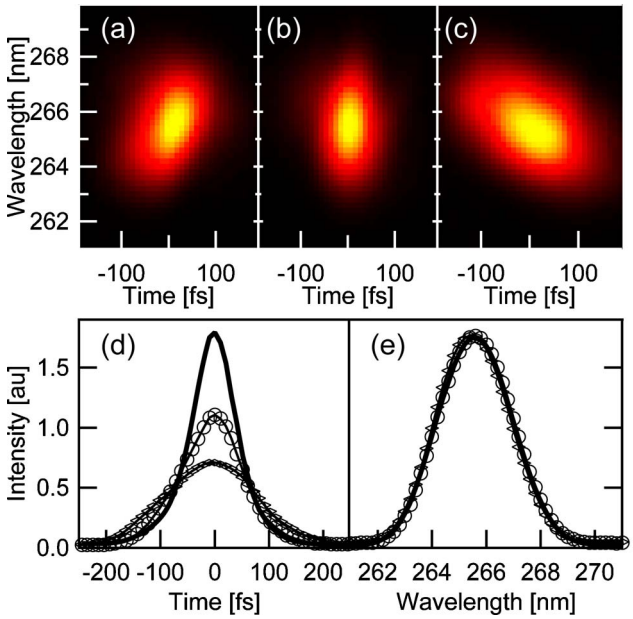

Fig. 5. (Color online) Effect of quadratic phase modulation compressing the (c) originally upchirped pulse to a (b) short, unchirped pulse, to a (a) down-chirped at $\lambda_0 = 400$ nm. Corresponding (d) cross correlations and (e) spectra extracted from XFROG are depicted by (a) circles, (b) line, and (c) lozenges.

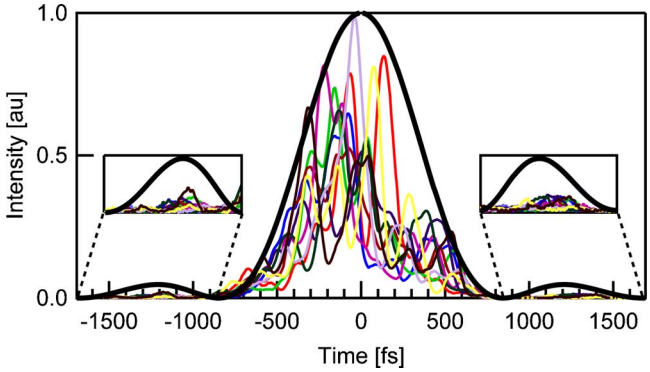

Fig. 6. (Color online) Multicolored lines (online), cross-correlations obtained ten different random spectral phase masks at $\lambda_0 = 400$ nm. Black line, theoretical shaping window [23] for the given spectral resolution. Insets, position of the first replica [22].

pulse while the spectrum remains unchanged, demonstrating the absence of phase-to-amplitude coupling via diffraction [16].

In Fig. 5(c), we demonstrate the functionality at $\lambda_0 = 400$ nm by applying a 10π-folded parabolic phase pattern [Fig. 1(b)]. A -1500 fs^2 correction was applied to compensate for the positive chirp introduced on the UV pulse by the optical elements of the setup. By increasing the quadratic phase modulation to -3770 fs^2, we reversed the chirp sign [Fig. 5(a)]. The corresponding cross correlations are shown in Fig. 5, again, and notably, for this kind of reflective pixelated devices [16], the spectra even for this wavelength remained unchanged upon modulation [Fig. 5(e)].

Figure 6 illustrates the possible pulse train complexity at 400 nm. We recorded cross correlations of ten random phase masks applied on the SLM (color lines), superimposed by the theoretical shaping window (thick line). The insets magnify the pulse intensities at the position of the first replicas at ± 1.3 ps, in agreement with theoretical calculations [22].

In conclusion, we have demonstrated phase modulation in the UV and the near-IR using our newly developed reflective SLM. Assuming $\lambda/15$ as a limit for the surface flatness acceptance, the device could be used for phase shaping of femtosecond pulses in an unprecedented wavelength range ranging from 225 nm up to 6 μm if the inner, flatter region is considered.

We are grateful to Michel Moret, P.-A. Clerc, Fabio Jutzi, Sébastien Lani, Michael Canonica, Peter Brühlmeier, Altatec AG, and the staff of the CSEM cleanroom facilities. We acknowledge the financial support of the Swiss National Science Foundation (SNSF) (contract 200020-124689/1), Swiss SER (COST MP0603), and the NCCR QP8.

[†]These authors contributed equally to this work.

References

1. R. S. Judson and H. Rabitz, Phys. Rev. Lett. **68**, 1500 (1992).
2. M. Dantus and V. V. Lozovoy, Chem. Rev. **104**, 1813 (2004).
3. J. L. Herek, W. Wohlleben, R. J. Cogdell, D. Zeidler, and M. Motzkus, Nature **417**, 533 (2002).
4. V. I. Prokhorenko, A. M. Nagy, S. A. Waschuk, L. S. Brown, R. R. Birge, and R. J. D. Miller, Science **313**, 1257 (2006).
5. M. Roth, L. Guyon, J. Roslund, V. Boutou, F. Courvoisier, J. P. Wolf, and H. Rabitz, Phys. Rev. Lett. **102**, 253001 (2009).
6. C. H. Tseng, S. Matsika, and T. C. Weinacht, Opt. Express **17**, 18788 (2009).
7. R. Selle, P. Nuernberger, F. Langhojer, F. Dimler, S. Fechner, G. Gerber, and T. Brixner, Opt. Lett. **33**, 803 (2008).
8. M. Roth, M. Mehendale, A. Bartelt, and H. Rabitz, Appl. Phys. B **80**, 441 (2005).
9. B. J. Pearson and T. C. Weinacht, Opt. Express **15**, 4385 (2007).
10. S. Weber, M. Barthelemy, and B. Chatel, Appl. Phys. B **98**, 323 (2010).
11. N. Krebs, R. A. Probst, and E. Riedle, Opt. Express **18**, 6164 (2010).
12. T. Tanigawa, Y. Sakakibara, S. B. Fang, T. Sekikawa, and M. Yamashita, Opt. Lett. **34**, 1696 (2009).
13. M. Hacker, G. Stobrawa, R. Sauerbrey, T. Buckup, M. Motzkus, M. Wildenhain, and A. Gehner, Appl. Phys. B **76**, 711 (2003).
14. K. W. Stone, M. T. W. Milder, J. C. Vaughan, and K. A. Nelson, in *Ultrafast Phenomena XV* (Springer, 2007), Vol. 88.
15. Y. Esumi, M. D. Kabir, and F. Kannari, Opt. Express **17**, 19153 (2009).
16. A. Rondi, J. Extermann, L. Bonacina, S. M. Weber, and J. P. Wolf, Appl. Phys. B **96**, 757 (2009).
17. J. Mohring, T. Buckup, C. S. Lehmann, and M. Motzkus, J. Opt. Soc. Am. B **26**, 1538 (2009).
18. L. Y. Lin, J. L. Shen, S. S. Lee, G. D. Su, and M. C. Wu, in *Mems 97, Proceedings—IEEE, Tenth Annual International Workshop on Micro Electro Mechanical Systems* (IEEE, 1997).
19. S. M. Weber, J. Extermann, W. Noell, F. Jutzi, S. Lani, D. Kiselev, L. Bonacina, N. F. de Rooij, and J. P. Wolf, Proc. SPIE **7594**, 75940J (2010).
20. O. E. Martinez, J. Opt. Soc. Am. B **3**, 929 (1986).
21. R. Trebino, K. W. DeLong, D. N. Fittinghoff, J. N. Sweetser, M. A. Krumbugel, B. A. Richman, and D. J. Kane, Rev. Sci. Instrum. **68**, 3277 (1997).
22. M. M. Wefers and K. A. Nelson, J. Opt. Soc. Am. B **12**, 1343 (1995).
23. A. M. Weiner, Rev. Sci. Instrum. **71**, 1929 (2000).